Ketamine Rapidly Enhances Glutamate-Evoked Dendritic Spinogenesis in Medial Prefrontal Cortex Through Dopaminergic Mechanisms

Supplementary Information

Mingzheng Wu, Samuel Minkowicz, Vasin Dumrongprechachan, Pauline Hamilton, Yevgenia Kozorovitskiy

Supplemental Methods and Materials

Mouse strains and genotyping

Animals were handled according to protocols approved by the Northwestern University Animal Care and Use Committee. Weanling and young adult male and female mice (postnatal days 25-60) were used in this study. Approximately equal numbers of males and females were used for every experiment. All mice were group-housed, with standard feeding, light-dark cycle, and enrichment procedures; littermates were randomly assigned to conditions. C57BL/6 mice used for breeding and backcrossing were acquired from Charles River (Wilmington, MA), and all other mouse lines were acquired from the Jackson Laboratory (Bell Harbor, ME) and bred in house.

B6.SJL-Slc6a3$^{tm1.1(cre)Bkmn}$/J mice, which express Cre recombinase under control of the dopamine transporter promoter, are referred to as DAT^{iCre} (1); B6.FVB(Cg)-Tg(Drd1-cre)FK150Gsat/Mmucd mice, which express Cre recombinase under control of the dopamine Drd1a receptor promoter, are referred to as Drd1^{Cre}(FK150) (2); Drd1$^{tm2.1Stl}$ floxed mutant mice that possess loxP sites flanking the single exon of the Drd1a gene, are referred to as Drd1^{ff} (3). All transgenic animals were backcrossed to C57BL/6 for several generations. Heterozygous Cre^{+} mice were used in experiments. Standard genotyping primers are available on the Jackson Lab website.

Stereotactic injections and optic fiber implants

Conditional expression of target genes in Cre-containing neurons was achieved using recombinant adeno-associated viruses (AAVs) using the FLEX cassette or encoding a double-floxed inverted open reading frame (DIO) of target genes, as described previously (4). For chemogenetic experiments in mPFC, Drd1^{Cre}(FK150) mice were transduced with AAV1.CBA.DIO.rM3Ds.mCherry.WPRE (4.3x10^{13} GC/ml, packaged by Vigene Biosciences). rM3Ds.mCherry sequence (Addgene #50458, Dr. Bryan Roth) was cloned into pAAV-CBA-DIO backbone (Addgene #81008, Dr. Bernardo Sabatini) (5) between AscI and NheI restriction sites. For chemogenetic inhibition of DA terminals in mPFC, DAT^{iCre} mice were transduced with a custom built AAV1.CBA.DIO.hM4Di.mCherry (1.28 x 10^{13} GC/ml, Vigene Biosciences, Rockville, MD, plasmid a gift from Dr. Bernardo Sabatini) (5). For glutamate uncaging-evoked spinogenesis experiments, AAV8.CAG.FLEX.EGFP (3.1 x 10^{12} GC/ml, UNC vector core, Dr. Ed Boyden) was co-injected with AAV1.hSyn.Cre.WPRE.hGH (1 x 10^{10}, UPenn viral core, Dr. James M. Wilson, unpublished) to achieve sparse expression in mPFC pyramidal neurons of C57BL/6 or Drd1^{ff} mice. To achieve cell-autonomous inhibition of PKA via expression of PKIα in mPFC, AAV1.FLEX.PKIα.IRES.nls.mRuby2 (1.35x10^{13} GC/ml, packaged by Vigene Biosciences, Addgene #63059) (6) was co-injected with AAV1.hSyn.Cre.WPRE.hGH and AAV8.CAG.FLEX.EGFP. For optogenetics experiments, DAT^{iCre} mice were transduced with AAV1.EF1a.DIO.hChR2(H134R).eYFP (3.55 x 10^{13} GC/ml), acquired from Dr. Karl Deisseroth (Addgene viral prep #20298-AAV1), or AAV8.CAG.FLEX.EGFP for controls.

Neonatal viral transduction was carried out to minimize invasiveness and increase surgical efficiency (4,7–10). P3-6 mice were cryoanesthetized, received ketoprofen for analgesia, and were placed on a cooling pad. Virus was delivered at a rate of 100 nl/min for up to 150-200 nl using an UltraMicroPump (World Precision Instruments, Sarasota, FL). Medial prefrontal cortex (mPFC) was targeted in the neonates by directing the needle immediately posterior to the eyes, 0.3 mm from midline, and 1.8 mm ventral to skin surface. Ventral tegmental area (VTA) was targeted in the neonates by directing the needle approximately ±0.2 mm lateral from Lambda and 3.8 mm ventral to skin surface. Coordinates were slightly adjusted based on pup age and size. Following the procedure, pups were warmed on a heating pad and returned to home cages.

For optogenetics in the mPFC, custom-made optical fibers were used (2 mm stub length, 200 µm diameter, 0.5 NA, FP200ERT, Thorlabs). Coordinates for mPFC fiber placement were +2.0 mm (AP), +0.4 mm (ML), and 1.3 - 1.6 mm (DV). For bilateral cannulation in mPFC: +2.2 mm (AP); 1.2 mm (DV), with center to center distance of 0.8 mm. Dummy cannulae with projections of 0.2 mm over the guide cannulae (2.5 mm) were inserted after implantation. Internal cannulae with projections of 0.5 mm were used for liquid delivery. Behavioral experiments were conducted 7-12 days after implantation.

Behavior assays

Learned helplessness (LH). To evaluate the effect of ketamine on learned helplessness behavior, a single dose of ketamine (10 mg/kg b.w., i.p.) was given 48 hrs after the last induction session, and the test session was performed 4 hrs later. For chemogenetic activation of rM3Ds in mPFC, 48 hrs after the last induction session, Clozapine N-oxide (CNO) was administered i.p., followed by test sessions 4 hrs and 24 hrs later. For chemogenetic inhibition of DA terminals in mPFC, the first CNO dose (3 mg/kg, i.p.) was co-administered with ketamine 48 hrs after the last induction, followed by test sessions 4 and 24 hrs later. Then, immediately following the last test session ketamine was administered alone, followed by test sessions 4, 24, and 72 hrs later. For optogenetic activation of DA terminals in the mPFC, 48 hrs after the last induction session a test session was performed with optogenetic stimulation. Bursts were not time-locked to behavior and consisted of ten 20 ms long pulses at 20 Hz, with 500 ms long burst duration and 10 sec inter-burst intervals. Optical power of light at the tip of fiber was <9 mW/mm^2. Light stimulation was applied in either compartment of the shuttle box.

Locomotion test. To assess the locomotor activity, mice were placed in the center of a plastic chamber (48 cm × 48 cm × 40 cm) or in the shuttle box in a dimly lit room. Mice explored the arena for 15 min, with video (30 fps) and photometry recording performed during the final 10 min.

All behavioral assays were conducted during the active phase of the circadian cycle.

Local drug infusion

To inhibit hM4Di-expressing DA terminals by local CNO infusion in mPFC, we used internal cannulae (28 gauge, Plastics One, Roanoke, VA) with 0.5 mm long projection beyond the implanted guide-cannula, as described above. 1 mM CNO (1 µL per side) was administered over a 2 min long injection period using a 10 µl Hamilton syringe (Hamilton Company, Franklin, MA). Dummy cannulae with 0.2 mm projection were inserted back after the delivery of CNO. The first infusion was performed immediately before ketamine injection, and the two subsequent infusions were performed 1.5 and 3 hrs after ketamine injection. Learned helplessness behavior was assessed 4 and 24 hours after ketamine treatment. In separate groups of animals, local CNO infusion was performed 24 hours after ketamine treatment, and learned helplessness behavior was tested 2 hours after infusion.

Acute slice preparation

Coronal brain slice preparation was modified from previously published procedures (4,7,11). Animals were deeply anesthetized by inhalation of isoflurane, followed by a transcardial perfusion with ice-cold, oxygenated artificial cerebrospinal fluid (ACSF) containing (in mM) 127 NaCl, 2.5 KCl, 25 $NaHCO_3$, 1.25 NaH_2PO_4, 2.0 $CaCl_2$, 1.0 $MgCl_2$, and 25 glucose (osmolarity 310 mOsm/L). After perfusion, the brain was rapidly removed, and immersed in ice-cold ACSF equilibrated with 95%O_2/5%CO_2. Tissue was blocked and transferred to a slicing chamber containing ice-cold ACSF, supported by a small block of 4% agar (Sigma-Aldrich). Bilateral 300 µm-thick slices were cut on a Leica VT1000s (Leica Biosystems, Buffalo Grove, IL) in a rostro-caudal direction and transferred into a holding chamber with ACSF, equilibrated with 95%O_2/5%CO_2. Slices were transferred to a recording chamber perfused with oxygenated ACSF at a flow rate of 2–4 ml/min at room temperature.

Pharmacology

Pharmacological agents were acquired from Tocris (Bristol, UK) or Sigma-Aldrich (St. Louis, MO). *In vivo* injections included intraperitoneal and subcutaneous injections of ketamine (10 mg/kg, Vedco, St. Joseph, MO), SKF 83566 (10 mg/kg, Tocris), Clozapine N-oxide (3 mg/kg *in vivo*, Sigma-Aldrich). SKF 81297 hydrobromide (SKF 81297, 1 µM, Tocris), and H-89 dihydrochloride (H-89, 10 µM, Tocris) were used in acute slice experiments, as noted.

Tissue processing and immunohistochemistry

Mice were deeply anaesthetized with isoflurane and transcardially perfused with 4% paraformaldehyde (PFA) in 0.1 M phosphate buffered saline (PBS). Brains were post-fixed for 1-5 days and washed in PBS, prior to sectioning at 50-100 µm on a vibratome (Leica Biosystems). Sections were pretreated in 0.2% Triton X-100 for an hour at RT, then blocked in 10% bovine serum albumin (BSA, Sigma-Aldrich, ST Louis, MO):PBS with 0.05%

Triton X-100 for two hours at RT, and incubated for 24-48 hrs at 4°C with primary antibody solution in PBS with 0.2% Triton X-100. On the following day, tissue was rinsed in PBS, reacted with secondary antibody for 2 hrs at RT, rinsed again, then mounted onto Superfrost Plus slides (ThermoFisher Scientific, Waltham, MA). Sections were dried and coverslipped under ProLong Gold antifade reagent with DAPI (Molecular Probes, Life Technologies, Carlsbad, CA) or under glycerol:TBS (9:1) with Hoechst 33342 (2.5µg/ml, ThermoFisher Scientific). Primary antibodies used in the study were mouse anti-tyrosine hydroxylase (1:1000; AB129991, Abcam, Cambridge, UK), chicken anti-GFP (1:2000; AB13970, Abcam, Cambridge, UK), rabbit anti-RFP (1:500, 600-401-379, Rockland, Limerick, PA), and rabbit anti-pCREB S133 (1: 5000, Abcam, ab32096). Alexa Fluor 488-, Fluor 594-, or Fluor 647-conjugated secondary antibodies against rabbit, mouse, or chicken (Life Technologies, Carlsbad, CA) were diluted 1:500. Whole sections were imaged with an Olympus VS120 slide scanning microscope (Olympus Scientific Solutions Americas, Waltham, MA). Confocal images were acquired with a Leica SP5 confocal microscope (Leica Microsystems). Depth-matched z-stacks of 2 µm-thick optical sections were analyzed in ImageJ (FIJI) (12,13). For pCREB quantification, every four adjacent z stack slices were combined, for a total of 6 µm thickness. mCherry signal was used to localize cell bodies of rM3Ds-expressing neurons. Laser intensity and all imaging parameters were held constant across samples, and the same threshold was applied for subtracting background immunofluorescence. $pCREB^{+}$ neurons were identified by an experimenter blind to the conditions.

Quantitative fluorescence *in situ* hybridization

Quantitative fluorescence *in situ* hybridization (FISH) was conducted following previously published procedures(11,14). Mice were deeply anesthetized by inhalation of isoflurane and decapitated. Brains were quickly removed and frozen in tissue-freezing medium on a mixture of dry ice and ethanol for 5 - 15 min prior to storage at 80°C. Brains were subsequently cut on a cryostat (Leica CM1850, Leica Biosystems) into 20 µm-thick sections, adhered to Superfrost Plus slides, and frozen at 80°C. Samples were fixed with 4% PFA in 0.1 M PBS at 4°C for 15 min, processed according to the manufacturer's instructions in the RNAscope Fluorescent Multiplex Assay manual for fresh frozen tissue (Advanced Cell Diagnostics, Newark, CA), and coverslipped with ProLong Gold antifade reagent with DAPI (Molecular Probes). Enhanced green fluorescent protein channel 1 (*Egfp*) and dopamine Drd1a receptor channel 2 (*Drd1a*) probes were added to slides in combination, and Amp4-b fluorescent amplification reagent was used for all experiments. Sections were subsequently imaged on a Leica SP5 confocal microscope in four channels with a 40x objective lens at a zoom of 1.4 and resolution of 512 x 512 pixels with 1.0 µm between adjacent z sections. Images were taken across the entire population of mPFC *Egfp*-positive neurons in each brain section.

FISH images were analyzed using FIJI (12). Briefly, every four adjacent z stack slices were combined, for a total of 3 µm thickness, in order to minimize missed colocalization, while decreasing false positive colocalization

driven by signal from cells at a different depth in a similar x-y position. All channels were thresholded. Cellular ROIs were defined using the *Egfp*$^{+}$ channel information to localize cell bodies. FISH molecule puncta were counted within established cell boundaries. Whether a cell was considered positive for a given marker was determined by setting a transcript-dependent threshold of the number of puncta (e.g., over 5 puncta/soma for *Drd1a*$^{+}$). These stringent parameters for co-localization and the challenges of quantifying low abundance receptor transcripts likely lead to underestimation of receptor-positive populations.

Supplementary Figures

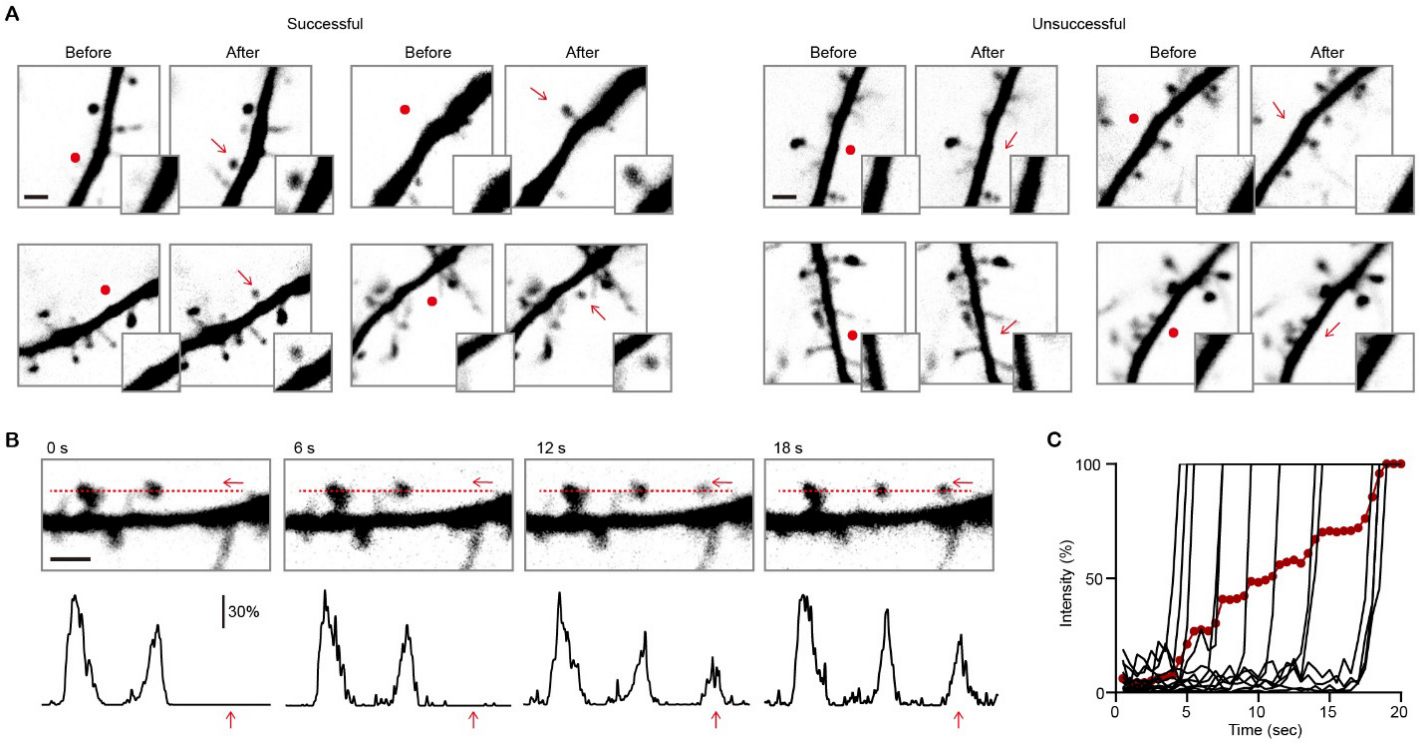

Supplementary Figure S1. *De novo* glutamate-induced spinogenesis on pyramidal neurons in mPFC

(A). Example 2PLSM images of successful and unsuccessful induction trials of *de novo* spinogenesis. Red circles, uncaging sites. Inset, close up images of local dendritic segments before and after glutamate uncaging. Scale bar, 2 μm.

(B). Top, time-lapse images of spine formation during glutamate uncaging (40 pulses, 2 Hz). Red arrow, uncaging spot and nascent spine. Line-scan analysis was performed, as noted by the red dashed line. Bottom, fluorescence intensity profiles from the line-scan across pre-existing spines and uncaging spot. Scale bar, 2 μm.

(C). Time course of individual trials (2 Hz) and average (red dots) fluorescence intensity changes across a series of successful trials during glutamate uncaging.

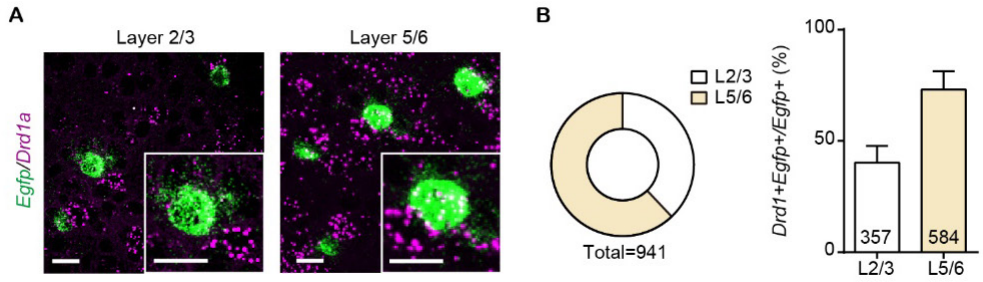

Supplementary Figure S2. *Drd1a* mRNA expression and distribution in mPFC

(A). Fluorescence in situ hybridization (FISH) image showing Drd1a mRNA in Egfp mRNA expressing cells in layer 2/3 and layer 5/6 of mPFC. Inset, close up of a single neuron. Scale bar, 20 μm.

(B). Left, the proportional distribution of Egfp mRNA expression across superficial and deep cortical layers. Right, quantification of the percentage of Drd1a+ cells among Egfp+ cells in superficial and deep cortical layers. n = 4 animals; Drd1+Egfp+/Egfp+: Layer 2/3, 40.2% ± 7.5%, layer 5/6, 73.1% ± 8.3%.

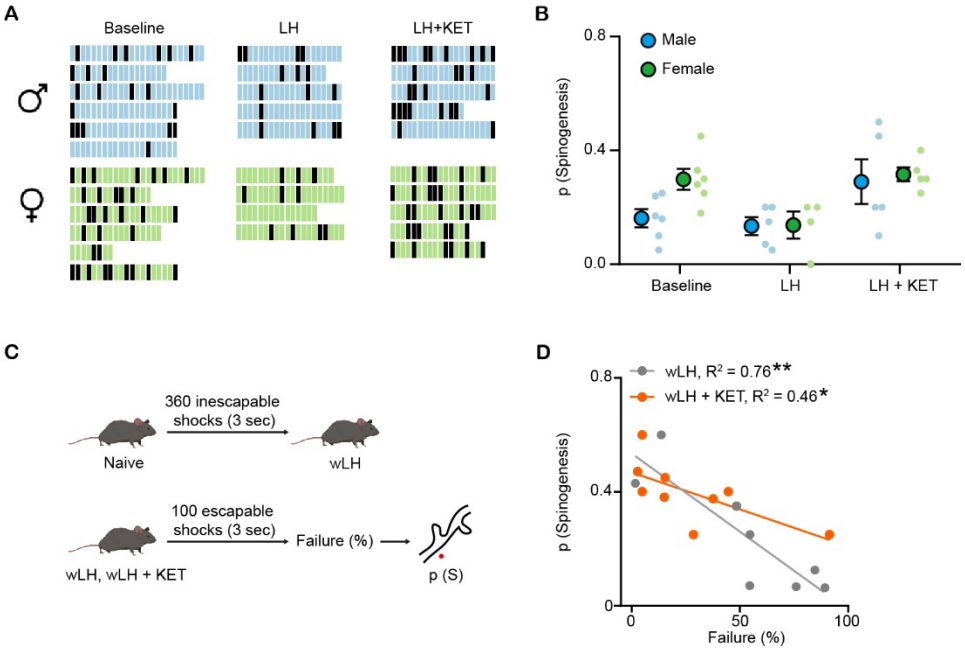

Supplementary Figure S3. Spinogenesis in mPFC is regulated by stress and correlates with behavioral outcomes

(A). Binary grid plots illustrating sequences of spinogenesis induction outcomes for different mice in all conditions in Figure 2c, separated by sex. Black, successful evoked spinogenesis trial; blue or green, unsuccessful trial for males or females, respectively.

(B). Probability of glutamate-evoked spinogenesis on deep layer mPFC neurons in conditions (baseline, LH, LH + KET) in male and female mice. Two-way ANOVA, Row factor (sex), $p = 0.1408$. Column factor (condition), $p = 0.0052$. Sidak's multiple comparison test, Male vs Female, Baseline, $p = 0.0775$, LH and LH + KET, $p > 0.9$, n = 4-6 animals as shown in individual dots. Error bars reflect SEM.

(C). Schematic illustrating wLH paradigm and glutamate-evoked spinogenesis assay after wLH and wLH + KET in separate groups of mice.

(D). Correlation between failures to escape and the probability of spinogenesis after learning and following ketamine treatment. wLH, $R^2 = 0.76$, $p = 0.0051$, n = 8 animals. wLH + KET, $R^2 = 0.46$, $p = 0.0439$, n = 9 animals.

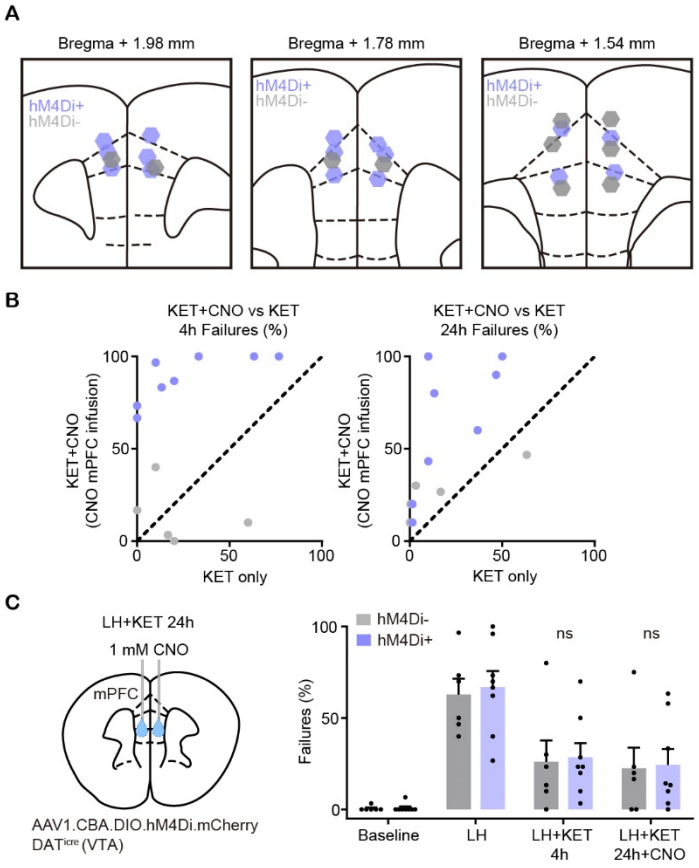

Supplementary Figure S4. Effects of local inhibition of DA terminals in mPFC

(A). Atlas locations showing cannula placements for data in Figure 4H.

(B). Within subject summary data for behavioral responses (Figure 4H) after ketamine treatment, compared with ketamine + CNO (mPFC), 4 hrs and 24 hrs after treatment, n = 5 – 8 animals.

(C). Left, schematic illustrating local CNO infusion in mPFC 24 hrs after ketamine treatment. Right, summary data showing the percentage of failures to escape an escapable aversive shock across learning and treatment conditions for hM4Di-expressing DAT^{iCre} positive and negative animals. Behaviors were tested 2 hrs after local CNO infusion. n = 6 animals for Cre-, 8 animals for Cre+, two-way ANOVA, Sidak's multiple comparison test, $p > 0.9$ for all comparisons.

Supplemental References

1. Bäckman CM, Malik N, Zhang YJ, Shan L, Grinberg A, Hoffer BJ, *et al.* (2006): Characterization of a mouse strain expressing Cre recombinase from the 3′ untranslated region of the dopamine transporter locus. *Genesis* 44: 383–390.

2. Gong S, Doughty M, Harbaugh CR, Cummins A, Hatten ME, Heintz N, Gerfen CR (2007): Targeting Cre recombinase to specific neuron populations with bacterial artificial chromosome constructs. *J Neurosci* 27: 9817–23.

3. Sariñana J, Kitamura T, Künzler P, Sultzman L, Tonegawa S (2014): Differential roles of the dopamine 1-class receptors, D1R and D5R, in hippocampal dependent memory. *Proc Natl Acad Sci U S A* 111: 8245–8250.

4. Kozorovitskiy Y, Peixoto R, Wang W, Saunders A, Sabatini BL (2015): Neuromodulation of excitatory synaptogenesis in striatal development. *Elife* 4: e10111.

5. Hou XH, Hyun M, Taranda J, Huang KW, Todd E, Feng D, *et al.* (2016): Central Control Circuit for Context-Dependent Micturition. *Cell* 167: 73-86.e12.

6. Chen Y, Saulnier JL, Yellen G, Sabatini BL (2014): A PKA activity sensor for quantitative analysis of endogenous GPCR signaling via 2-photon FRET-FLIM imaging. *Front Pharmacol* 5: 56.

7. Kozorovitskiy Y, Saunders A, Johnson CA, Lowell BB, Sabatini BL (2012): Recurrent network activity drives striatal synaptogenesis. *Nature* 485: 646–650.

8. Peixoto RT, Wang W, Croney DM, Kozorovitskiy Y, Sabatini BL (2016): Early hyperactivity and precocious maturation of corticostriatal circuits in Shank3B−/− mice. *Nat Neurosci* 19: 716–724.

9. Bariselli S, Tzanoulinou S, Glangetas C, Prévost-Solié C, Pucci L, Viguié J, *et al.* (2016): SHANK3 controls maturation of social reward circuits in the VTA. *Nat Neurosci* 19: 926–934.

10. He CX, Arroyo ED, Cantu DA, Goel A, Portera-Cailliau C (2018): A Versatile Method for Viral Transfection of Calcium Indicators in the Neonatal Mouse Brain. *Front Neural Circuits* 12. https://doi.org/10.3389/fncir.2018.00056

11. Xiao L, Priest MF, Nasenbeny J, Lu T, Kozorovitskiy Y (2017): Biased Oxytocinergic Modulation of Midbrain Dopamine Systems. *Neuron* 95: 368-384.e5.

12. Schindelin J, Arganda-Carreras I, Frise E, Kaynig V, Longair M, Pietzsch T, *et al.* (2012): Fiji: an open-source platform for biological-image analysis. *Nat Methods* 9: 676–82.

13. Schneider CA, Rasband WS, Eliceiri KW (2012, July 28): NIH Image to ImageJ: 25 years of image analysis. *Nature Methods*, vol. 9. Nature Publishing Group, pp 671–675.

14. Xiao L, Priest MF, Kozorovitskiy Y (2018): Oxytocin functions as a spatiotemporal filter for excitatory synaptic inputs to VTA dopamine neurons. *Elife* 7: e33892.